

Comparison of relative signal-to-noise ratios of different classes of imaging spectrometer

R. Glenn Sellar and Glenn D. Boreman

The continued development of new and fundamentally different classes of imaging spectrometer has increased both the scope and the complexity of comparisons of their relative signal-to-noise ratios. Although the throughput and multiplex advantages of Fourier-transform spectrometers were established in the early 1950s, the application of this terminology to *imaging* spectrometers is often ambiguous and has led to some confusion and debate. For comparisons of signal-collection abilities to be useful to a system designer, they must be based on identical requirements and constraints. We present unambiguous definitions of terminology for application to imaging spectrometers and comparisons of signal-collection abilities and signal-to-noise-ratios on a basis that is useful to a systems designer and inclusive of six fundamentally different classes (both traditional and novel) of imaging spectrometers. © 2005 Optical Society of America

OCIS codes: 120.0280, 120.4570, 120.4640, 120.5630, 120.6200.

1. Introduction

Imaging spectrometers are designed to measure the energy or quanta collected from an object as a function of two spatial and one spectral dimension. Most modern imaging spectrometers employ two-dimensional detector arrays, which collect signal (in units of energy or quanta) as a function of column number, row number, and exposure number. To be useful, these raw data must be transformed from the image coordinate system of column, row, and exposure into the object coordinate system of cross-track position, along-track position, and wavelength (or wave number.)

Imaging spectrometers used for remote sensing may be divided into classes based on two criteria: the method by which they achieve spatial discrimination and the method by which they achieve spectral discrimination.¹ Methods of acquiring spatial information include whiskbroom, pushbroom, framing, and the rel-

atively new class that we refer to as windowing. A whiskbroom scanning instrument employs a zero-dimensional field of view (FOV) that scans the object in both the along-track and the cross-track directions; a pushbroom scanning instrument scans a one-dimensional FOV in the along-track direction only. A framing (also called staring) instrument employs a two-dimensional FOV that remains fixed on the object during acquisition. We use "framing" as synonymous with "staring" but prefer the former term because, if the scene to be observed is longer than the length of a single FOV, multiple acquisitions will be required; thus "framing" seems more descriptive. We use the term "windowing" to describe the relatively new class of instruments that employ a two-dimensional FOV that moves across the object in a continuous fashion in the along-track direction. Windowing is actually distinct from the time-delay integration technique used by some panchromatic imagers because in a windowing instrument a distinct exposure is acquired each time the FOV moves forward by a one ground sample and no integration occurs.

Methods of acquiring spectral information include the familiar filtering, dispersive, and interferometric techniques. Dispersive instruments may use either a prism or a grating. By "interferometric" we refer to Fourier-transform spectrometers (FTSs) that employ two-beam interferometers such as the Michelson, Mach-Zehnder, and Sagnac. Multiple-beam interferometers such as the Fabry-Perot have signal-collection abilities that are more similar to those of

When this work was done, R. G. Sellar (glenn.sellar@jpl.nasa.gov) was with the Department of Physics, University of Central Florida, Orlando, Florida. He is now with the Jet Propulsion Laboratory, Mail Stop 171-B1, 4800 Oak Grove Drive, Pasadena, California 91109. G. D. Boreman is with the Center for Research and Education in Optics and Lasers/School of Optics, University of Central Florida, Orlando, Florida 32816-2700.

Received 19 January 2004; revised manuscript received 22 June 2004; accepted 19 November 2004.

0003-6935/05/091614-11\$15.00/0

© 2005 Optical Society of America

Table 1. Classification of Imaging Spectrometers

Type of Spectral Scanner	Along-Track Scanning		
	Pushbroom	Windowing	Framing
Filtering	No known examples	Filter array Wedge filter Linear variable filter	Band-sequential Filter wheel Tunable filter ^a
Dispersive	Grating or prism	(No known examples)	Image slicer Tomographic
Interferometric	Static FTS (Sagnac)	Static FTS (Mach-Zehnder, Sagnac)	Traditional FTS (Michelson)

^aAcousto-optical tunable filter or liquid-crystal tunable filter.

filtering instruments than of FTSs. This classification scheme, with examples of commonly used terms for each class, is illustrated in Table 1.

The signal-collection abilities of spectrometers depend in part on the throughput, or etendue (product of area and solid angle), and the spectral bandwidth. Although the corresponding throughput and multiplex advantages of FTSs were established in the early 1950s (by Jacquinot and Dufour² and Jacquinot^{3,4} and by Fellgett,^{5,6} respectively), the application of these concepts to imaging spectrometers is complex and has been a subject of debate.^{7,8} To be useful to a system designer, intercomparisons of the relative signal-to-noise-ratios (SNRs) provided by different classes of imaging spectrometer must be based on a common set of requirements and constraints. The key requirements are the performance requirements of spatial and spectral range and resolution. The key constraints are the characteristics of the object to be observed, the time available to complete the observation, and the detector technology. Careful definition of a common basis for comparison is required to allow for useful comparisons of the SNRs among instruments that acquire data in fundamentally different ways.

2. Basis for Comparison

A useful comparison of instruments must be based on identical performance requirements and identical constraints for each instrument. We define the performance requirements as the spatial sampling intervals (ground sample distances) across track and along track; the number of spatial samples across track and along track, denoted M_x and M_y , respectively; the spectral range; and the number of spectral samples. A specification of spectral resolution in constant-wavelength intervals would favor dispersive and filter instruments, whereas a specification of constant wave-number intervals would favor interferometric instruments, so we specify only the spectral range and the number of spectral samples, which is neutral. We use M_λ to denote the number of spectral samples.

Requirements on the swath width (extent of the object in the cross-track dimension) and the swath

length (extent of the object in the along-track dimension) derive from the required number of spatial samples and the required ground sample distances in the respective directions (swath width is the product of cross-track ground sample distance and number of cross-track samples, whereas swath length is the product of along-track ground sample distance and number of along-track spatial samples). The spectral range is the product of the spectral sampling interval and the number of spectral samples. This set of requirements common to each instrument is summarized in Table 2, along with typical units.

The common set of constraints comprises observation of the same object defined by its spectral radiance, observation from the same range, the same total time available to complete the acquisition task, use of identical detector arrays with M_i rows and M_j columns, and the same mass. The mass constraint may derive from limitations of the platform (typically an aircraft or spacecraft) and leads to a constraint on the aperture areas that is in any case required for a fair comparison. Note that the effective focal length is also consequently constrained by the required swath width and the width of the detector array. The number of exposures read from the array is not constrained. The constraints are summarized in Tables 3 and 4. The constraint of identical detector arrays is reasonable for the most usual combinations of M_y , M_λ , and M_j , but there are some cases where this constraint is not reasonable across every class of instrument. For a dispersive instrument with a fixed grating or prism, we require $M_j \geq M_\lambda$. For the framing classes, if $M_j > M_y$, then some pixels would be unused. Therefore if our comparison is to include the dispersive classes and the

Table 2. Common Set of Requirements

Dimension	Range	Sample Extent	Number of Samples
Cross track	X_o (m)	Δx_o (m)	M_x
Along track	Y_o (m)	Δy_o (m)	M_y
Spectral	Λ_o (μm)	$\Delta \lambda_o$ (μm)	M_λ
Temporal	τ (s)	τ (s)	l

Table 3. Detector Array Constraints in Common

Constraint	Array	Pixel	Number of Elements
Width	X_i (m)	Δx_i (m)	M_i
Height	Y_i (m)	Δy_i (m)	M_j
Detector Noise		N_d	

Table 4. Other Constraints in Common

Object spectral radiance	L_λ (photons $s^{-1} m^{-2} sr^{-1} \mu m^{-1}$)
Range to object	d (m)
Aperture	Constrained by mass limitation
Effective focal length	f (mm, derived from other constraints)

framing classes, we require $M_y \geq M_x$. This condition is usually met for applications of remote sensing to land or water, but may not be the case for remote sensing of the atmosphere.

3. Calculation of Relative Signal-to-Noise Ratio Factors

To calculate the relative SNRs one must first determine the relative signal levels. The signal is given by the following equation:

$$S = L_\lambda \eta A \Omega (\Delta \lambda) (\Delta \tau), \quad (1)$$

where S represents the signal [photons], L_λ is the spectral radiance [photons $s^{-1} m^{-2} sr^{-1} \mu m^{-1}$], η is the efficiency (dimensionless), A is the area [m^2], Ω is the solid angle [sr], $\Delta \lambda$ is the spectral extent [μm], and $\Delta \tau$ is the temporal extent [s]. Note that, although we use the symbol λ here, the spectral units could be either wavelength [μm] or wave number [cm^{-1}] as long as both the spectral radiance and the spectral extent use the same spectral units. Similarly, the signal could be specified in either energy or quanta as long as the spectral radiance is specified in the corresponding units. Also note that, in general, spectral radiance L_λ and efficiency η will be functions of wavelength, in which case Eq. (1) will be replaced by

$$S = \int L_\lambda(\lambda) \eta(\lambda) A \Omega (\Delta \tau) d\lambda. \quad (2)$$

As we shall be calculating relative signals here, we use Eq. (1), with the simplifying assumption of constant spectral radiance and constant efficiency.

The definition of radiance⁹ is such that, when losses are ignored, radiance is not a function of propagation distance. As long as all losses are accounted for in efficiency factor η , one may therefore use the same spectral radiance L_λ in calculating the signal at any space in the system, including the object space, the final image space, and even an intermediate image plane or a pupil plane.

The efficiency term η includes diffraction efficiency, interferometer rejection, and absorption, as appropri-

ate to each class of instrument. For the dispersive classes an antireflection-coated prism may permit an efficiency close to unity. Two-beam interferometers have two output apertures, and, although some designs allow both outputs to be used, we have used an efficiency of 1/2 for the interferometric classes on the assumption that only one output is used. An efficiency of 1/2 is also used for the filtering classes to account for absorption losses. These assigned values for η are summarized in Table 1. These approximate efficiencies are appropriate for first-order comparisons among classes of instrument; extension of these analyses to comparisons of detailed instrument designs could use more-specific values for η . The quantum efficiency of the detector has been ignored because the basis for comparison is that all instruments use the same detector array and the quantum efficiency will therefore cancel in the calculations of relative signal for different classes of instrument.

A. Signal from Each Object Voxel

We use the term “voxel” in imaging spectrometry to mean a single element in a three-dimensional space defined by two spatial and one spectral dimension. Thus an object voxel is a portion of the object bounded in the two spatial dimensions by the cross-track and along-track ground sample distances and in the spectral dimension by the spectral sampling interval. In this analysis we assume that there are no gaps or overlaps between samples in either the spatial or the spectral dimension. Using Eq. (1), we can write the signal collected from a single object voxel s_o as

$$s_o = L_\lambda \eta (\Delta x_o) (\Delta y_o) \Omega_o (\Delta \lambda_o) (\Delta \tau_o). \quad (3)$$

Equation (3) results from Eq. (1) as follows: $A = (\Delta x_o) (\Delta y_o)$ is the area of an object voxel where Δx_o is the spatial extent in the cross-track direction and Δy_o is the spatial extent in the along-track direction; Ω_o is the solid angle subtended by the entrance aperture of the instrument as viewed from the object; $\Delta \lambda_o$ is the spectral extent of a voxel; and $\Delta \tau_o$ is the temporal extent during which flux is collected from that particular voxel. We immediately note that the parameters L_λ , Δx_o , Δy_o , Ω_o , and $\Delta \lambda_o$ are all determined by the common set of requirements and constraints and thus are by definition identical for all classes of imaging spectrometer. In calculations of the relative signals for different classes of instrument these factors will cancel because they will have the same value for all classes. For the signal from a single object voxel, only efficiency η and temporal extent $\Delta \tau_o$ vary with the class of instrument.

Temporal extent parameter $\Delta \tau_o$ is the time span during which a voxel in the object is observed by the instrument. From the point of view of an imaging spectrometer, the object has three dimensions: two spatial and one spectral. Determination of $\Delta \tau_o$ therefore requires an understanding of the imaging spectrometer’s three-dimensional analog of a panchromatic imager’s two-dimensional FOV and of how this evolves with time. The FOV of a panchromatic

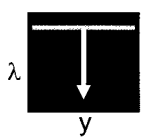
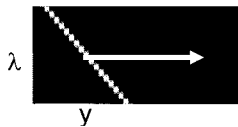


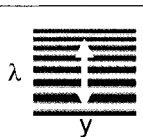
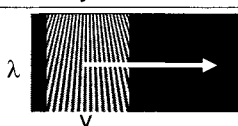
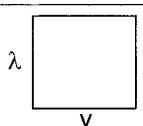
Spectral Class Scan Class	η	Transmittance vs. y and λ	$\Delta\tau_0$
Filtering (Framing)	$\left(\frac{1}{2}\right)$		$\frac{\tau}{M_\lambda} \left(\frac{M_j}{M_y}\right)$
Filtering (Windowing)	$\left(\frac{1}{2}\right)$		$\frac{\tau}{M_\lambda} \left(\frac{M_j}{M_y + M_j}\right)$
Dispersive (Pushbroom)	(1)		$\frac{\tau}{M_y}$
Interferometric (Pushbroom)	$\left(\frac{1}{2}\right)$		$\frac{\tau}{M_y}$
Interferometric (Framing)	$\left(\frac{1}{2}\right)$		$\tau \left(\frac{M_j}{M_y}\right)$
Interferometric (Windowing)	$\left(\frac{1}{2}\right)$		$\tau \left(\frac{M_j}{M_y + M_j}\right)$
Panchromatic (Framing)	(1)		$\tau \left(\frac{M_j}{M_y}\right)$

Fig. 1. Determination of efficiency η and temporal extent $\Delta\tau$ for an object voxel.

imager is a two-dimensional map of the object pixels that are observed by the imager at one point in time. Understanding of imaging spectrometers is facilitated by an extension of the concept of a FOV to include a third dimension (the spectral dimension). Thus the transmittance function of an imaging spectrometer is a three-dimensional map of the object voxels that are observed by the imaging spectrometer at one point in time. For all the imaging spectrometers considered in this paper, the transmittance does not vary with cross-track position x , so in Fig. 1 only two-dimensional side views of these three-dimensional transmittance functions are displayed, i.e., transmittance as a function of along-track position y and wavelength λ . This figure maps in white those voxels in the object that are observed at any instant in time and indicates with arrows the directions in which these maps evolve with time; determination of the respective $\Delta\tau_0$ factors are facilitated by the use of this figure.

The temporal extent $\Delta\tau_0$ of an object voxel (the time

during which an object voxel is within the transmittance function) is the product of three factors: the total time available to complete the observation, τ ; and a factor that depends on the spatial class and a factor that depends on the spectral class of the instrument. The transmittance function for a pushbroom instrument includes only those voxels at one of the M_y along-track sample positions at any time, so the time for which each voxel will be within the transmittance function includes a factor of $1/M_y$. The transmittance function for a framing instrument includes all those voxels at M_j along-track sample positions simultaneously; therefore the temporal extent for an object voxel in this case includes a factor of M_j/M_y . For a windowing instrument the transmittance function must be swept all the way across each ground sample,^{10,11} so in this case the spatial factor is $M_j/M_y + M_j$.

In a filtering instrument the transmittance function is further restricted to only those voxels at a single spectral sample, so the temporal extent of an

Table 5. Signal Factors and Example Relative Signals for an Object Voxel and for the Entire Object

Spectral Class (Scan Class)	Signal Factor	Relative Signal for Example: $M_y = 4000$, $M_\lambda = 200$, $M_j = 1000$
Filtering (Framing)	$\left(\frac{1}{2}\right)\left(\frac{1}{M_\lambda} \frac{M_j}{M_y}\right)$	2.5
Filtering (Windowing)	$\left(\frac{1}{2}\right)\left(\frac{1}{M_\lambda} \frac{M_j}{M_y+M_j}\right)$	1
Dispersive (Pushbroom)	$(1)\left(\frac{1}{M_y}\right)$	1
Interferometric (Pushbroom)	$\left(\frac{1}{2}\right)\left(\frac{1}{M_y}\right)$	0.5
Interferometric (Framing)	$\left(\frac{1}{2}\right)\left(\frac{M_j}{M_y}\right)$	500
Interferometric (Windowing)	$\left(\frac{1}{2}\right)\left(\frac{M_j}{M_y+M_j}\right)$	400
Panchromatic (Framing)	$(1)\left(\frac{M_j}{M_y}\right)$	1000

object voxel for a filtering instrument includes an additional factor of $1/M_\lambda$. Dispersive and interferometric instruments, however, accept all wavelengths simultaneously, so the spectral factor in $\Delta\tau_o$ is unity for these classes. Strictly speaking, the interferometric instruments reject an average of half of the spectral samples, but we have already accounted for this rejection by giving the value of efficiency η as $1/2$. We could instead have used an efficiency of unity and included a spectral factor of $1/2$ in the determination of $\Delta\tau_o$, to the same effect. The resultant temporal extents $\Delta\tau_o$ for each class are tabulated in Fig. 1, along with illustrations of the transmittance functions. The panchromatic framing class, although it is simply an imager rather than an imaging spectrometer, is included in Fig. 1 for purposes of comparison.

Having determined all the factors in the signal equation in terms of the requirements and constraints, we can now compare the signal-collection abilities of the different classes of imaging spectrometer. Table 5 shows the relative signal expected for each class. We derived the relative signals from Eq. (3) by canceling out the parameters that are the same for every class (L_λ , Δx_o , Δy_o , Ω_o , $\Delta\lambda_o$, and τ) and substituting the numerical values of η , leaving as variables only the required number of spectral samples M_λ , the required number of along-track spatial samples M_y , and the number of pixels in the array in the along-track orientation, M_j . A numerical example is also shown in Table 5 for a typical case with $M_y = 4000$, $M_\lambda = 200$, and $M_j = 1000$. The relative signals in the numerical example are normalized relative to the signal for the dispersive pushbroom class.

B. Signal from the Entire Object

The signal S_o obtained from the entire object is given by the product of the signal from each voxel s_o and the number of voxels $M = (M_x M_y M_\lambda)$:

$$\begin{aligned}
 S_o &= L_\lambda \eta (\Delta x) (\Delta y) \Omega (\Delta \lambda) (\Delta \tau) M \\
 &= L_\lambda \eta (\Delta x_o) (\Delta y_o) \Omega_o (\Delta \lambda) (\Delta \tau) M_x M_y M_\lambda \\
 &= L_\lambda \eta (\Delta x_o M_x) (\Delta y_o M_y) \Omega_o (\Delta \lambda M_\lambda) (\Delta \tau) \\
 &= L_\lambda \eta X_o Y_o \Omega_o \Lambda (\Delta \tau),
 \end{aligned} \tag{4}$$

where S_o is the signal from the entire object and the other terms are as defined in Tables 2 and 3. As was the case when the signal was calculated in the individual object voxels, the parameters L_λ , X_o , Y_o , Ω_o , and Λ are all determined by the common set of requirements and constraints and thus will cancel when one is calculating the relative signals for different classes of instrument. Once again we found that the only parameters that vary with the class of instrument are efficiency η and temporal extent $\Delta\tau_o$. The relative signal factors and the numerical example for the signal collected from the entire object will therefore be identical to those for the individual voxels, and thus the relative signals presented in Table 5 apply to both the signal from each individual object voxel and the signal collected from the entire object.

C. Signal in a Single Raw Data Element

Whereas the signal obtained from each object voxel is the signal of most relevance to the user of the data, we may also consider the signal obtained in each element of the raw data (before the raw data are transformed into the object coordinate system). We obtain this signal by performing the signal calculation in image space. Signal s_i in a single raw data element (one exposure of one pixel) is given by

$$s_i = L_\lambda \eta (\Delta x_i) (\Delta y_i) \Omega_i (\Delta \lambda_i) (\Delta \tau_i). \tag{5}$$

Equation (5) results from Eq. (1) follows: $A = (\Delta x_i) (\Delta y_i)$ is the area of a pixel where Δx_i is the spatial extent in the cross-track direction and Δy_i is the spatial extent in the along-track direction, Ω_i is the solid angle subtended by the exit pupil of the optics as viewed from the detector pixel, $\Delta\lambda_i$ is the spectral extent of the flux allowed to reach that pixel, and $\Delta\tau_i$ is the integration time for each exposure of the detector array. Note that the temporal extent of a data element $\Delta\tau_i$ is not the same as the temporal extent of an object voxel $\Delta\tau_o$. The temporal extent of an object voxel is the time during which a voxel in the object is observed as explained in the preceding sections, whereas the temporal extent of a data element in image space is the exposure time of the detector with which the data element is acquired.

We immediately note that the parameters L_λ , Δx_i , Δy_i , and Ω_i are all determined by a common set of requirements and constraints and thus are by definition identical for all classes of imaging spectrometer. For the signal in a single raw data element, only efficiency η , spectral extent $\Delta\lambda_i$, and temporal extent $\Delta\tau_i$ vary with the class of instrument. Also note that, although we have constrained the total acquisition time τ to be the same for each instrument, the number of exposures M_k and resultant individual exposure times $\Delta\tau_i$ are not constrained (a fair comparison

requires the total acquisition time to be the same, but there is no reason to require the number of exposures taken during that time to be the same for all instruments).

In a filtering spectrometer the filter restricts the spectral extent (bandwidth) at any point in time to the spectral extent of a single filter. Dispersive instruments spread the spectral range across the rows of the array, so a pixel on any particular row receives only a small fraction of the spectral range. Two-beam interferometers allow the entire spectral range to reach the elements in the image plane. In the case of the interferometric pushbroom class a cylindrical lens is used to spread the flux along the rows. This has an effect on the signal received by each image element that is radiometrically similar to effect of the grating or prism in the dispersive class. For convenience of presentation, we include the term that accounts for the effect of the cylindrical lens in the interferometric pushbroom class in place of the spectral extent term for the other classes.

The number of exposures M_k is not constrained to be the same for each class; only the total time available for acquisition τ is constrained. A filtering framing instrument must acquire at least one exposure for each spectral band, so $M_k \geq M_\lambda$ for this class of instrument. Pushbroom instruments must acquire one exposure for each along-track element, so $M_k \geq M_y$ in this case. To prevent aliasing, interferometric instruments must acquire at least two measurements for each spectral band, so $M_k \geq 2M_\lambda$ for interferometric framing instruments. Windowing instruments must first acquire one exposure for each row of the detector array and then one additional exposure for each along-track element in the object, so $M_k \geq M_j + M_y$ for the windowing classes. In remote sensing the required number of spatial elements M_y is usually much higher than the number of spectral bands M_λ , so typically $M_j + M_y \geq 2M_\lambda$, and we use $M_k = M_j + M_y$ here as the number of exposures for the windowing interferometric class. Spectral extent $\Delta\lambda$, number of exposures M_k , and temporal extent $\Delta\tau$ in image space for each class of instrument are listed in Table 6.

Having determined all the factors in the signal equation for a single element in image space, we can now predict the signal expected in each raw data element (one exposure of one pixel) for each of the different classes of imaging spectrometer. Table 7 shows the relative signal expected for each class. We derived the relative signals from Eq. (5) by canceling out the parameters that are the same for all classes (L_λ , Δx_i , Δy_i , Ω_i , and τ). A numerical example is also shown in Table 7 for the same (typical) parameters used in the example in Table 5: number of along-track samples, $M_y = 4000$; number of spectral samples, $M_\lambda = 200$; and number of rows in the detector array, $M_j = 1000$. The signals in the numerical example are normalized relative to the signal for the dispersive pushbroom class.

Table 6. Spectral Extent $\Delta\lambda_i$ for a Raw Data Element, Number of Exposures M_k , and Temporal Extent $\Delta\tau_i$ for a Raw Data Element

Spectral Class (Scan Class)	$\Delta\lambda_i$	M_k	$\Delta\tau_i$
Filtering (Framing)	$\frac{\Lambda}{M_\lambda}$	$M_\lambda \left(\frac{M_y}{M_j}\right)$	$\frac{\tau M_j}{M_\lambda M_y}$
Filtering (Windowing)	$\frac{\Lambda}{M_\lambda}$	$M_y + M_j$	$\frac{\tau}{M_y + M_j}$
Dispersive (Pushbroom)	$\frac{\Lambda}{M_j}$	M_y	$\frac{\tau}{M_y}$
Interferometric (Pushbroom)	$\frac{\Lambda}{M_j}$	M_y	$\frac{\tau}{M_y}$
Interferometric (Framing)	$\frac{\Lambda}{2}$	$2M_\lambda \left(\frac{M_y}{M_j}\right)$	$\frac{\tau M_j}{2M_\lambda M_y}$
Interferometric (Windowing)	$\frac{\Lambda}{2}$	$M_y + M_j$	$\frac{\tau}{M_y + M_j}$
Panchromatic (Framing)	Λ	$\frac{M_y}{M_j}$	$\frac{\tau M_j}{M_y}$

D. Signal in the Entire Set of Data Elements

The signal S accumulated in the entire set of data elements is given by the product of the signal from each data element s and the number of data elements M . In most cases the number of data elements is simply given by

$$M = M_i M_j M_k. \quad (6)$$

But, in the case of a windowing instrument, it must be noted that some data elements are collected from portions of the object that are outside the desired borders of the object and are therefore discarded. The number of data elements in the windowing case is therefore

Table 7. Signal Factors and Example Relative Signals for a Raw Data Element (Image Space)

Spectral Class (Scan Class)	Signal Factor	Relative Signal for Example: $M_y = 4000$, $M_\lambda = 200$, $M_j = 1000$
Filtering (Framing)	$\left(\frac{1}{2}\right)\left(\frac{1}{M_\lambda}\right)\left(\frac{M_j}{M_\lambda M_y}\right)$	12.5
Filtering (Windowing)	$\left(\frac{1}{2}\right)\left(\frac{1}{M_\lambda}\right)\left(\frac{1}{M_y + M_j}\right)$	2
Dispersive (Pushbroom)	$(1)\left(\frac{1}{M_j}\right)\left(\frac{1}{M_y}\right)$	1
Interferometric (Pushbroom)	$\left(\frac{1}{2}\right)\left(\frac{1}{M_j}\right)\left(\frac{1}{M_y}\right)$	0.5
Interferometric (Framing)	$\left(\frac{1}{2}\right)(1)\left(\frac{M_j}{2M_\lambda M_y}\right)$	5,000
Interferometric (Windowing)	$\left(\frac{1}{2}\right)(1)\left(\frac{1}{M_y + M_j}\right)$	400
Panchromatic (Framing)	$(1)(1)\left(\frac{M_j}{M_y}\right)$	1,000,000

Table 8. Number of Data Elements and Signal Factors for the Sum of all Data Elements (Image Space)

Spectral Class (Scan Class)	M	Signal Factor
Filtering (Framing)	$M_i M_\lambda M_y$	$\left(\frac{1}{2}\right) \left(\frac{1}{M_\lambda} \frac{M_j}{M_y}\right)$
Filtering (Windowing)	$M_i M_j M_y$	$\left(\frac{1}{2}\right) \left(\frac{1}{M_\lambda} \frac{M_j}{M_y + M_j}\right)$
Dispersive (Pushbroom)	$M_i M_j M_y$	$(1) \left(\frac{1}{M_y}\right)$
Interferometric (Pushbroom)	$M_i M_j M_y$	$\left(\frac{1}{2}\right) \left(\frac{1}{M_y}\right)$
Interferometric (Framing)	$M_i 2M_\lambda M_y$	$\left(\frac{1}{2}\right) \left(\frac{M_j}{M_y}\right)$
Interferometric (Windowing)	$M_i M_j M_y$	$\left(\frac{1}{2}\right) \left(\frac{M_j}{M_y + M_j}\right)$
Panchromatic (Framing)	$M_i M_y$	$(1) \left(\frac{M_j}{M_y}\right)$

$$M = M_i M_j M_k - M_i M_j M_j. \quad (7)$$

For pushbroom and framing instruments the signal S_i in the entire set of data elements is given by

$$\begin{aligned} S_i &= L_\lambda \eta (\Delta x) (\Delta y) \Omega (\Delta \lambda) (\Delta \tau) M \\ &= L_\lambda \eta (\Delta x_i) (\Delta y_i) \Omega_i (\Delta \lambda_i) (\Delta \tau_i) M_i M_j M_k \\ &= L_\lambda \eta (\Delta x_i M_i) (\Delta y_i M_j) \Omega_i (\Delta \lambda_i) (\Delta \tau_i M_k) \\ &= L_\lambda \eta X_i Y_i \Omega_i (\Delta \lambda_i) \tau, \end{aligned} \quad (8)$$

whereas for windowing instruments we have

$$\begin{aligned} S_i &= L_\lambda \eta (\Delta x) (\Delta y) \Omega (\Delta \lambda) (\Delta \tau) M \\ &= L_\lambda \eta (\Delta x_i) (\Delta y_i) \Omega_i (\Delta \lambda_i) (\Delta \tau_i) (M_i M_j M_k - M_i M_j M_j) \\ &= L_\lambda \eta (\Delta x_i M_i) (\Delta y_i M_j) \Omega_i (\Delta \lambda_i) (\Delta \tau_i) (M_k - M_j) \\ &= L_\lambda \eta X_i Y_i \Omega_i (\Delta \lambda_i) (\tau - \Delta \tau M_j), \end{aligned} \quad (9)$$

where S_i is the signal from the entire object and the other terms are as defined above. The terms X_i and Y_i are the dimensions of the detector array, and $\Delta \tau_i M_k = \tau$, so for most classes the only parameters that vary with class are efficiency η and the range of wavelengths allowed to reach a single pixel, $\Delta \lambda_i$. For the windowing classes there is also a difference in the temporal term, but this variation is minor compared to the variations in the spectral terms for the different classes. The number of data elements and the relative signals for the sum of all data elements for each class of instrument are listed in Table 8.

We note that the relative signal factors for individual image elements are not in general the same as the relative signal factors for individual object elements, but this is not surprising because the number of raw data elements differs with class. Calculations of the signal collected from the entire object, however, give exactly the same result whether they are performed

in object space or in image space, as one may see by comparing Table 5 with Table 8.

E. Discussion of Relative Signals

When performing calculations of signals in object space one may be surprised to find no difference between classes in the etendue term ($A\Omega$)—which one might generally associate with the expected throughput advantage of interferometric windowing and interferometric framing imaging spectrometers—but to find instead that the signals differ in the temporal ($\Delta\tau$) term. Similarly, one may be surprised to find that for calculations of signal in a raw data element (image space) the most influential factor is the spectral term ($\Delta\lambda$). If one looks to find somewhere a throughput advantage, one may find it by considering the total signal when the calculation is performed either in an intermediate image space or in the space of the exit pupil. In an intermediate image space the field mask (slit) employed in the pushbroom classes will restrict the areal term (A), whereas in the exit pupil space the slit will restrict the solid angular term (Ω), either of which one would generally associate with the throughput advantage.

The absence of a throughput advantage for the interferometric classes when one is calculating the signal from a single object voxel in an imaging spectrometer is in agreement with previous findings.^{7,8} Our analysis has shown, however, that an advantage in signal will be present regardless of the space in which the signal calculation is performed. In Ref. 8, only the rate at which photons are collected (in units of photons/s) rather than the actual collected signals (in units of photons), is compared. By thus ignoring how the temporal term in Eq. (1) varies with the class of instrument, one misses the key difference between instruments. In Eq. (3) the terms L_λ , Δx_o , Δy_o , Ω_o , and $\Delta \lambda_o$ are constrained by the common set of performance requirements and constraints, and therefore the rate at which photons are emitted from a single object voxel that has a radiance L_λ and dimensions Δx_o , Δy_o , and $\Delta \lambda_o$ will be the same regardless of the type of instrument used to collect these photons. If the instruments are constrained to have the same mass, the apertures will be roughly the same size and Ω_o will be the same for every class. The only remaining terms in Eq. (3) are efficiency η and temporal term $\Delta \tau_o$. The most significant differences among classes of instrument are in the temporal term: the length of time during which photons from an individual object voxel are detected by the instrument. If one compares only the signal rates, one misses this most important factor, which controls the relative signal collected by different classes of imaging spectrometer. Rather than the signal alone, of course, it is the SNR that is the more relevant figure of merit. In addition to the differences in signal, there are also important differences in the effects of noise on the different classes—which we address below—but, for a comparison of the resultant SNRs to be correct, the calculation of the signals must first be correct.

The absence of a throughput advantage in some

calculations is therefore an issue of the terminology used rather than of the relative signal-collection abilities. Although the terms “Jaquinot’s advantage” and “throughput advantage” are commonly used interchangeably, use of the term “throughput advantage” can lead to confusion. Strictly speaking, Jacquinot’s advantage is freedom from the requirement for an entrance slit. Only when the signal calculation is performed in the space of the intermediate image plane (where the slit defines areal term A) or in the space of the exit pupil (where the slit defines solid-angular term Ω) is the association with the throughput or etendue ($A\Omega$) clear. Calculation of the signal, however, may alternatively be performed in the image space, where the width of the slit defines the spectral extent term $\Delta\lambda_i$, or in the object space, where the width of the slit defines the temporal extent term $\Delta\tau_o$.

When calculations of signal are performed in image space, the most influential differences between classes appear in the spectral term, and this has sometimes led to the higher signal collected by interferometric classes being attributed incorrectly to the Fellgett or multiplex advantage.⁸ Fellgett’s advantage is, strictly speaking, the absence of the requirement for an exit slit. Whereas interferometric spectrometers (both imaging and nonimaging) do benefit from this advantage, the advent of one-dimensional detector arrays extended Fellgett’s advantage to dispersive nonimaging spectrometers and the advent of two-dimensional detector arrays extended it to dispersive imaging spectrometers as well, so the Fellgett advantage is moot. The importance of this point goes beyond terminology. For example, in Ref. 8 when a dispersive pushbroom instrument is compared to an interferometric framing instrument, a multiplex advantage factor of M_λ is attributed to the interferometric framing instrument. As we have pointed out here, however, both of these instruments possess the multiplex advantage (both are equipped with two-dimensional detector arrays rather than an exit slit). The correct distinction between these classes is that the framing classes have Jacquinot’s advantage (no entrance slit) whereas the pushbroom classes do not, and the correct relative signal factors for a single raw data element are those derived here and listed in Table 7.

As we have shown, although the term in the signal equation that is controlled by the entrance slit (temporal, areal, solid-angular, or spectral) depends on the space in which the calculation is performed, the advantage in signal provided by the interferometric windowing and interferometric framing classes is nevertheless actually due to Jacquinot’s advantage: the absence of an entrance slit. Therefore we suggest that, to avoid confusion, the terms throughput advantage and multiplex advantage not be used (at least not in reference to imaging spectrometers). Jacquinot’s advantage does pertain but may lead to confusion if it is used interchangeably with throughput advantage. Signal advantage would perhaps be a less-confusing term.

Finally, it should be noted that both the dispersive and the interferometric classes enjoy an advantage relative to the filtering classes, i.e., freedom from the requirement for a bandpass filter, and that this last advantage is distinct from both Jacquinot’s advantage (no entrance slit) and Fellgett’s advantage (no exit slit).

F. Noise

Determination of the SNRs requires that we address the noise as well as the signal. Here we distinguish between two categories of noise: signal-dependent noise and signal-independent noise. The primary form of signal-dependent noise is photon noise N_p , which is related to signal S by¹²

$$N_p = \sqrt{S}. \quad (10)$$

The primary source of signal-independent noise is detector noise, so we use the symbol N_d for this component of the noise, though in general this term may be taken to include all sources of noise that are independent of the signal. Recall that one of the constraints that we employ to form the basis for comparison among different classes of instrument is the use of identical detector arrays.

Total noise N is then simply given by

$$N = N_p + N_d. \quad (11)$$

G. Signal-to-Noise Ratios

For the filtering and the dispersive classes, the SNR is simply

$$\text{SNR} = \frac{S}{N} = \frac{S}{N_p + N_d}. \quad (12)$$

For the interferometric classes the SNR in the derived spectrum, SNR_s , is related to the SNR in the interferogram, SNR_i , by

$$\text{SNR}_s(\lambda) = \text{SNR}_i \left\{ \left[\frac{S(\lambda)}{\bar{S}} \right] \sqrt{\frac{1}{M_\lambda}} \right\}, \quad (13)$$

where $\text{SNR}_s(\lambda)$ is the SNR at wavelength λ in the derived spectrum, SNR_i is the SNR in the interferogram (i.e., in the raw data), and $S(\lambda)/\bar{S}$ is the ratio of the signal in a particular spectral band to the average signal over all of the M_λ spectral bands.^{13–15}

H. Relative Signal-to-Noise-Ratio Factors for Negligible Detector Noise

One special case for SNR is that of the photon noise limit, for which $N_d \ll N_p$. Application of Eqs. (10), (12), and (13) when $N_d = 0$ to the relative signal factors in Table 5 produces the relative SNR factors shown in Table 9. These general SNR factors provide a systems designer with a relevant comparison of the SNRs for each of the different classes of instrument

Table 9. SNR Factors for an Object Voxel

Spectral Class (Scan Class)	SNR Factor for $Q = 0$ (No Detector Noise)	SNR Factor for General Case
Filtering (Framing)	$\left[\left(\frac{1}{2}\right)\left(\frac{1}{M_\lambda} \frac{M_j}{M_y}\right)\right]^{1/2}$	$\frac{\left(\frac{1}{2}\right)\left(\frac{1}{M_\lambda} \frac{M_j}{M_y}\right)}{Q + \left[\left(\frac{1}{2}\right)\left(\frac{1}{M_\lambda} \frac{M_j}{M_y}\right)\right]^{1/2}}$
Filtering (Windowing)	$\left[\left(\frac{1}{2}\right)\left(\frac{1}{M_\lambda} \frac{M_j}{M_y + M_j}\right)\right]^{1/2}$	$\frac{\left(\frac{1}{2}\right)\left(\frac{1}{M_\lambda} \frac{M_j}{M_y + M_j}\right)}{Q + \left[\left(\frac{1}{2}\right)\left(\frac{1}{M_\lambda} \frac{M_j}{M_y + M_j}\right)\right]^{1/2}}$
Dispersive (Pushbroom)	$\left[(1)\left(\frac{1}{M_y}\right)\right]^{1/2}$	$\frac{(1)\left(\frac{1}{M_y}\right)}{Q + \left[(1)\left(\frac{1}{M_y}\right)\right]^{1/2}}$
Interferometric (Pushbroom)	$\left\{\left[\frac{S(\lambda)}{\bar{S}}\right]\sqrt{\frac{1}{M_\lambda}}\right\}\left[\left(\frac{1}{2}\right)\left(\frac{1}{M_y}\right)\right]^{1/2}$	$\left\{\left[\frac{S(\lambda)}{\bar{S}}\right]\sqrt{\frac{1}{M_\lambda}}\right\}\frac{\left(\frac{1}{2}\right)\left(\frac{1}{M_y}\right)}{Q + \left[\left(\frac{1}{2}\right)\left(\frac{1}{M_y}\right)\right]^{1/2}}$
Interferometric (Framing)	$\left\{\left[\frac{S(\lambda)}{\bar{S}}\right]\sqrt{\frac{1}{M_\lambda}}\right\}\left[\left(\frac{1}{2}\right)\left(\frac{M_j}{M_y}\right)\right]^{1/2}$	$\left\{\left[\frac{S(\lambda)}{\bar{S}}\right]\sqrt{\frac{1}{M_\lambda}}\right\}\frac{\left(\frac{1}{2}\right)\left(\frac{M_j}{M_y}\right)}{Q + \left[\left(\frac{1}{2}\right)\left(\frac{M_j}{M_y}\right)\right]^{1/2}}$
Interferometric (Windowing)	$\left\{\left[\frac{S(\lambda)}{\bar{S}}\right]\sqrt{\frac{1}{M_\lambda}}\right\}\left[\left(\frac{1}{2}\right)\left(\frac{M_j}{M_y + M_j}\right)\right]^{1/2}$	$\left\{\left[\frac{S(\lambda)}{\bar{S}}\right]\sqrt{\frac{1}{M_\lambda}}\right\}\frac{\left(\frac{1}{2}\right)\left(\frac{M_j}{M_y + M_j}\right)}{Q + \left[\left(\frac{1}{2}\right)\left(\frac{M_j}{M_y + M_j}\right)\right]^{1/2}}$
Panchromatic (Framing)	$\left[(1)\left(\frac{M_j}{M_y}\right)\right]^{1/2}$	$\frac{(1)\left(\frac{M_j}{M_y}\right)}{Q + \left[(1)\left(\frac{M_j}{M_y}\right)\right]^{1/2}}$

for any given set of performance requirements and constraints. Inspection of the variables in these factors also provides some intuition as to how the relative SNR factors for the photon-noise-limited case depend on the performance requirements and constraints. For the photon-noise-limited case the relative SNR factors for the filtering framing, filtering windowing, interferometric framing, and interferometric windowing classes contain a factor $\sqrt{M_j}$ in the numerator (this is essentially the result of freedom from the requirement for a slit, i.e., of the Jacquinot advantage). All classes other than the dispersive pushbroom class include a factor $\sqrt{M_\lambda}$ in the denominator.

I. Relative Signal-to-Noise-Ratio Factors for Nonnegligible Detector Noise

It is not, however, always practical to reach the limit of $N_d \ll N_p$. Detectors for the infrared often have substantial detector noise unless they are cooled to sufficiently low temperatures. Under some conditions thermal emission from the instrument itself is also

significant unless additional parts of the instrument are also cooled. For instruments that are limited in mass or power, such as those employed from small aircraft or spacecraft, cooling to arbitrarily low temperatures may not be practical. Thus a systems designer must at times design for conditions other than the ideal case of $N_d \ll N_p$, and it is therefore important also to illustrate the case in which the detector noise is nonnegligible.

To formulate useful expressions for the SNR factors for this general case we require a basis or reference for the detector noise that is relevant to all classes of imaging spectrometer. As our basis for comparison prescribes the use of identical detector arrays as well as a constraint of similar limitations on the mass of the instruments, we use the same value of N_d for each class. Recalling Eq. (3), which predicts the signal collected from a single object voxel, we note again that the parameters L_λ , Δx_o , Δy_o , Ω_o , and $\Delta \lambda_o$ are identical for all classes of imaging spectrometer and that only efficiency η and temporal extent $\Delta \tau$ vary with the class of instrument. The maximum

Table 10. Example Relative SNRs for an Object Voxel

Spectral Class (Scan Class)	Relative SNR for Example: $M_y = 4000$, $M_\lambda = 200$, $M_j = 1000$, $S(\lambda)/\bar{S} = 1$	
	$Q = 0$	$Q = 0.1$
Filtering (Framing)	1.6	2.3
Filtering (Windowing)	1.4	1.9
Dispersive (Pushbroom)	1	1
Interferometric (Pushbroom)	0.05	0.04
Interferometric (Framing)	1.6	9.0
Interferometric (Windowing)	1.4	7.9
Panchromatic (Framing)	32	193

possible value of η is of course unity, and the maximum possible value of $\Delta\tau_o$ is τ . Setting the parameters $\eta = 1$ and $\Delta\tau_o = \tau$ in Eq. (3) therefore predicts the signal from a single object voxel for an ideal instrument, i.e., an instrument that rejects none of the available photons. This ideal signal level may then be used as a reference for example values of N_d that have general relevance to all classes of imaging spectrometer. We define a noise-condition parameter Q such that

$$N_d = Q[L_\lambda A_o \Omega_o (\Delta\lambda_o) \tau]^{1/2}. \quad (14)$$

When $Q = 0$ we have the photon-noise-limited case, when $Q = 1$ the detector noise will be equal to the photon noise for an ideal instrument, and when $Q \gg 1$ we have the detector-noise-limited case. Using Eqs. (10), (12), and (14) yields the SNR factors for the general case $\text{SNR}_{\text{fac}}(Q)$:

$$\text{SNR}_{\text{fac}}(Q) = \frac{S_{\text{fac}}}{Q + \sqrt{S_{\text{fac}}}}, \quad (15)$$

where S_{fac} is the signal factor from Table 5.

The SNR factors for both the special case of $Q = 0$ (no detector noise) and the general case are presented in Table 9. We list numerical examples of the relative SNRs when $Q = 0$ (no detector noise) and when $Q = 0.1$ in Table 10, using parameters that may be considered fairly typical for many applications of imaging spectrometry in remote sensing: $M_y = 4000$, $M_\lambda = 200$, $M_j = 1000$, and $S(\lambda)/\bar{S} = 1$. The SNR factors for this example are plotted in Fig. 2 as a function of noise-condition parameter Q . Relative SNRs—normalized to the SNR factor for the dispersive pushbroom class—are shown in Fig. 3.

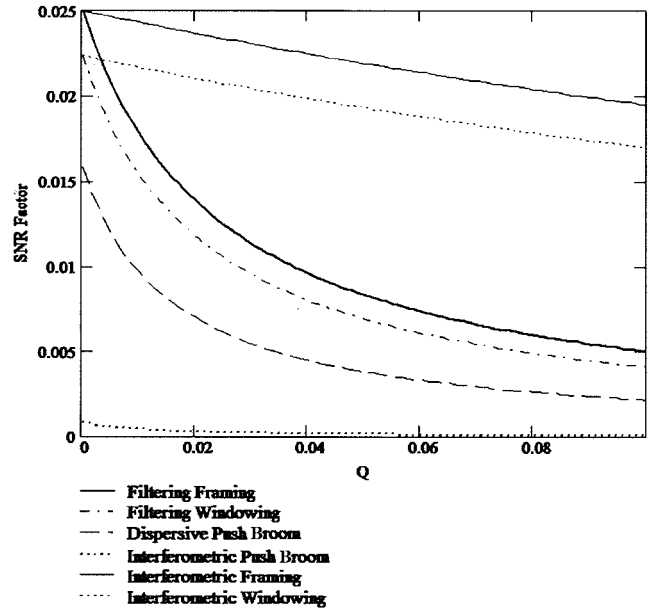


Fig. 2. Example SNR factors for an object voxel as a function of noise-condition parameter Q for $M_y = 4000$, $M_\lambda = 200$, $M_j = 1000$, and $S(\lambda)/\bar{S} = 1$.

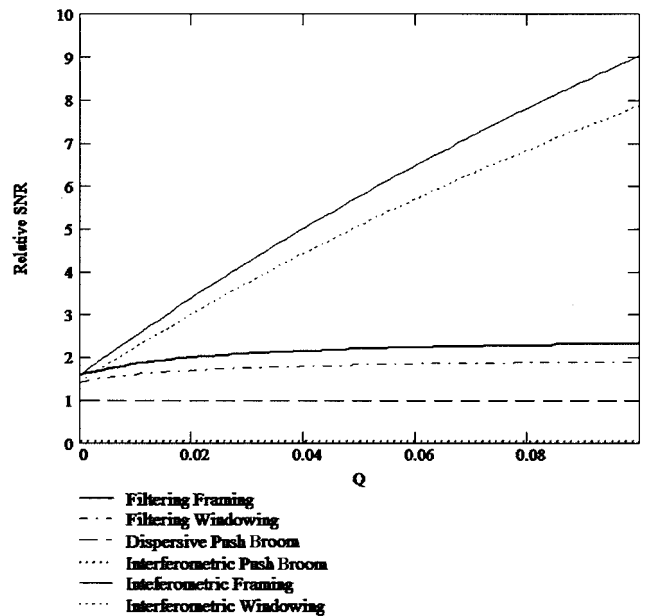


Fig. 3. Relative SNRs—normalized to the SNR for the dispersive pushbroom class—for an object voxel as a function of noise-condition parameter Q for the example $M_y = 4000$, $M_\lambda = 200$, $M_j = 1000$, and $S(\lambda)/\bar{S} = 1$.

4. Conclusions

The term in the signal equation from which the advantage in signal results depends on the space in which the calculation is performed. We therefore recommend use of the term “signal advantage” rather than “throughput advantage” for comparing the signal-collection abilities of different classes of imaging spectrometer.

The equations in Table 9 predict the relative SNR for each class of imaging spectrometer for any given set of requirements and constraints and therefore provide a valuable tool for the use of systems designers to determine which class of instrument will provide the highest SNR for their particular applications.

This research was funded by NASA under grant NAG5-10730.

References

1. R. G. Sellar and G. D. Boreman, "Classification of imaging spectrometers for remote sensing applications," *Opt. Eng.* (to be published).
2. P. Jacquinot and C. Dufour, "Condition optique d'emploi des cellules photo-électriques dans les spectrographes et les interféromètres," *J. Rech. Centre Nat. Rech. Sci. Lab. Bellevue* **6**, 91–103 (1948).
3. P. Jacquinot, "The etendue advantage," presented at the Seventeenth XVII Meeting of Congrès du Groupement avancement des méthodes d'analyse spectrométriques (Paris, 1954).
4. P. Jacquinot, "Caractères communs aux nouvelles méthodes de spectroscopie interférentielle; facteur de mérite," *J. Phys. Radium* **19**, 223–229 (1958).
5. P. B. Fellgett, "The multiplex advantage," Ph.D. dissertation (University of Cambridge, Cambridge, UK, 1951).
6. P. B. Fellgett, "Multi-channel spectrometry," *J. Opt. Soc. Am.* **42**, 872 (1952).
7. M. R. Descour, "Throughput advantage in imaging Fourier-transform spectrometers," in *Imaging Spectrometry II*, M. R. Descour and J. M. Mooney, eds., Proc. SPIE **2819**, 285–290 (1996).
8. L. W. Schumann and T. S. Lomheim, "Infrared hyperspectral imaging Fourier transform and dispersive spectrometers: comparison of signal-to-noise based performance," in *Imaging Spectrometry VII*, M. R. Descour and S. S. Shen, eds., Proc. SPIE **4480**, 1–14 (2002).
9. E. L. Dereniak and G. D. Boreman, *Infrared Detectors and Systems* (Wiley, New York, 1996), pp. 45–48.
10. J. C. Demro, R. Hartshorne, and L. M. Woody, "Design of a multispectral, wedge filter, remote sensing instrument incorporating a multi-port, thinned, CCD area array," in *Imaging Spectroscopy*, M. R. Descour, J. M. Mooney, D. L. Perry, and L. R. Illing, eds., Proc. SPIE **2480**, 280–294 (1995).
11. R. F. Horton, "Optical design for a high-etendue imaging Fourier-transform spectrometer," in *Imaging Spectrometry II*, M. R. Descour and J. M. Mooney, eds., Proc. SPIE **2819**, 300–315 (1996).
12. Ref. 9, p. 165.
13. F. D. Kahn, "The signal-noise ratio of a suggested spectral analyzer," *Astrophys. J.* **129**, 518–521 (1959).
14. S. P. Davis, M. C. Abrams, and J. W. Brault, *Fourier Transform Spectrometry* (Academic, New York, 2001).
15. P. J. Miller and A. R. Harvey, "Signal to noise analysis of various imaging systems," in *Biomarkers and Biological Spectral Imaging*, G. H. Bearman, D. J. Bornhop, and R. M. Levenson, eds., Proc. SPIE **4259**, 16–21 (2001).